# Bidirectional Elongation Strategy Using Ambiphilic Radical Linchpin for Modular Access to 1,4-Dicarbonyls via Sequential Photocatalysis

Akira Matsumoto,*,† Natsumi Maeda,† and Keiji Maruoka*,†,‡

†Graduate School of Pharmaceutical Sciences, Kyoto University, Sakyo, Kyoto 606-8501, Japan

‡School of Chemical Engineering and Light Industry, Guangdong University of Technology, Guangzhou 510006, China

*KEYWORDS: photoredox catalysis • sequential photocatalysis • phosphonium ylides • ambiphilic linchpin*

**ABSTRACT:** Organic molecules that can be connected with multiple substrates by sequential C–C bond formations can be utilized as linchpins in multicomponent processes. While they are useful for rapidly increasing molecular complexity, most of the reported linchpin coupling methods rely on the use of organometallic species as strong carbon nucleophiles to form C–C bonds, which narrows the functional group compatibility. Here, we describe a metal-free, radical-mediated coupling approach using a formyl-stabilized phosphonium ylide as a multifunctional linchpin under visible-light photoredox conditions. The present method uses the ambiphilic character of the phosphonium ylide, which serves both as a nucleophilic and an electrophilic carbon-centered radical source. The stepwise and controllable generation of these radical intermediates allows sequential photocatalysis involving two mechanistically distinct radical additions, both of which are initiated by the same photocatalyst in one pot with a high functional-group tolerance. The methodology enables a bidirectional assembly of the linchpin with two electronically differentiated alkene fragments and thus offers a rapid and modular access to 1,4-dicarbonyl compounds as versatile synthetic intermediates.

## INTRODUCTION

Rapid assembly of widely available substrates into synthetically valuable products is of prime importance in modern organic chemistry.[1] The use of small organic molecules that can be connected with multiple substrates by a sequential C–C bond-forming process has offered a bidirectional approach to increase molecular complexity with high modularity (Figure 1a).[2] Such multicomponent protocols utilizing linchpin compounds have enabled the expeditious construction of complex building blocks for natural products and biologically important molecules.[3] However, their C–C bond-forming processes rely heavily on using organometallic reagents as strong nucleophiles, which narrows the scope of accessible products due to limited functional group compatibility. Moreover, complicated manipulations (i.e., cryogenic conditions with the strict prohibition of water) are frequently required to control the reactivity of these reagents and intermediates. On the other hand, the chemistry of radical species can provide a complementary approach to that of ionic species for new bond disconnections.[4] The recent advances in methodologies for the generation of radical species, such as photoredox catalysis[5] and electrocatalysis,[6] have made these conditions milder and more practical. Despite these breakthroughs, the linchpin coupling strategy based on radical-mediated C–C bond formations has been less explored.[7]

Aliphatic aldehydes are one of the simplest linchpin motifs with ambiphilic character: While the formyl carbon is electrophilic, the α-carbon center can be a nucleophile via an enolate or enamine intermediate (Figure 1b). To date, several classic transformations associated with carbonyl groups, such as aldol reaction, Mannich reaction, and Wittig olefination, have been applied as methods for C–C bond formation with an aldehyde linchpin.[8] Similarly, in the field of radical chemistry, two different carbon-centered radicals can be generated from aldehydes. For example, hydrogen-atom transfer (HAT) from the formyl C–H bond affords nucleophilic acyl radicals.[9,10] On the other hand, single-electron transfer (SET) with various carbonyl compounds and their derivatives generates electrophilic radicals at the α-carbon of the carbonyl group.[11,12] Based on this background, we envisioned that the controlled activation of a specific aldehyde would unleash its latent reactivity both as a nucleophilic and an electrophilic carbon-centered radical in a sequential manner, thus functioning as an ambiphilic radical linchpin. Here, we report the realization of this concept by using (triphenylphosphoranylidene)acetaldehyde (**P1**) as a commercially available aldehyde to initiate these two mechanistically distinct radical processes (Figure 1c). With a single photoredox catalyst (PC), a one-pot sequence involving two different radical addition reactions via the formation of intermediate ylide **P2** was established by a stepwise and controllable generation of nucleophilic and electrophilic carbon-centered radicals. This approach allows modular access to 1,4-dicarbonyls, which are versatile synthetic intermediates and ubiquitous motifs found in natural products,[13] from two electronically differentiated alkene fragments. The mild and practical conditions of visible-light photoredox catalysis enable a rapid assembly of complex molecules with various functional groups, which are otherwise difficult to use with a polar linchpin coupling strategy.

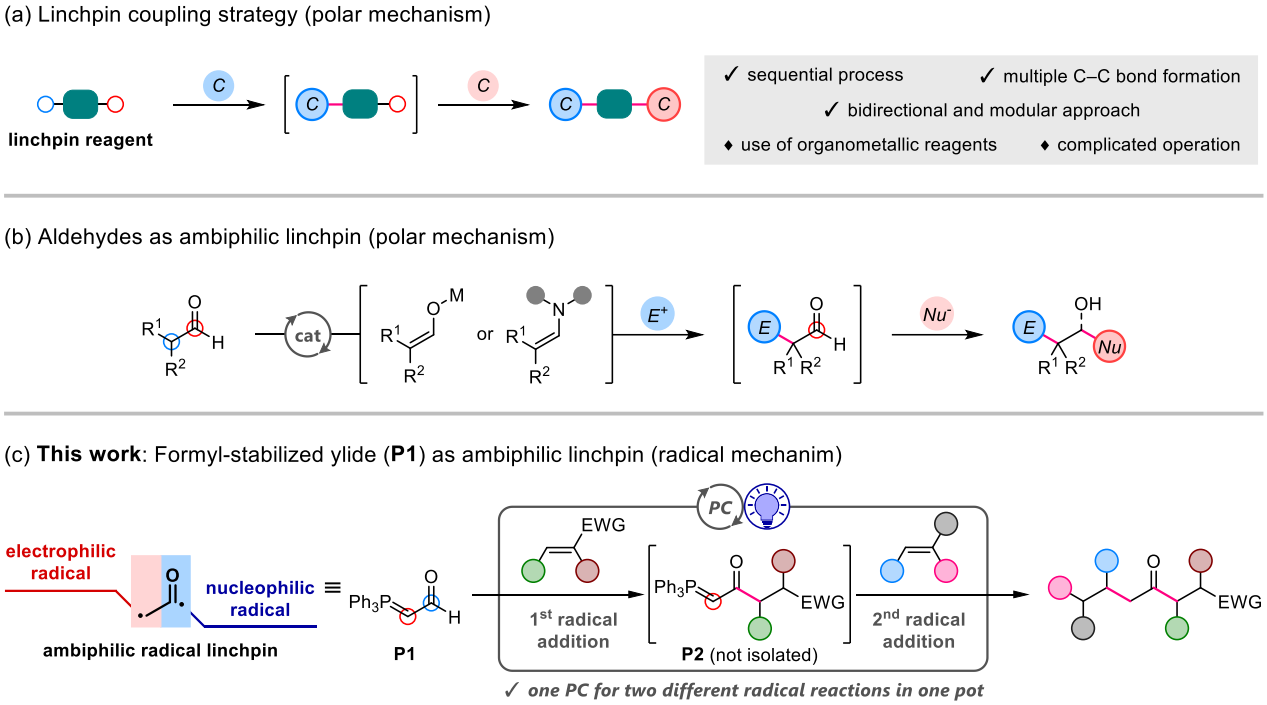


**Figure 1.** (a) General scheme for linchpin coupling strategy. (b) Aliphatic aldehydes as ambiphilic linchpins. (c) Sequential photocatalysis using formyl-stabilized phosphonium ylide (**P1**) as an ambiphilic radical linchpin. EWG = electron-withdrawing group.

## RESULTS AND DISCUSSION

**Optimization of Reaction Conditions.** We commenced our study by investigating the reactivity of **P1** as a precursor of a nucleophilic acyl radical. Initially, it was expected that the desired acyl radical would be generated via photoinduced HAT catalysis.[10,14] To our surprise, a brief survey of the conditions revealed that the reaction of **P1** and benzyl acrylate (**1a**) afforded the desired product **P2a** *in the absence of any HAT catalyst*. Further screening of photocatalysts led us to find 4CzIPN as the optimal catalyst (Table 1, entry 1. See the Supporting Information (SI) for details). Other catalysts with similar redox properties to 4CzIPN, such as 3CzClIPN and {[Ir[dF(CF$_3$)ppy]$_2$(dtbbpy)}PF$_6$ ([Ir]-2), also afforded high yields of **P2a**, while the strongly reducing catalyst (*fac*-Ir(ppy)$_3$: [Ir]-1) or the oxidizing catalyst (Me-Acr$^+$) were not effective (Table 1, entries 2–5). The use of other solvents, including DMSO, $CH_2Cl_2$, and acetone, showed lower efficiency than MeCN (Table 1, entries 6–8). Several control experiments and radical-trapping experiments by TEMPO (2,2,6,6-tetramethylpiperidine-1-oxyl) suggested a radical mechanism via excitation of the photocatalyst induced by visible light (Table 1, entries 9–10). We then investigated the scope of Michael acceptors. Although the purifications of the resulting ylides **P2** were difficult, a wide range of acceptors, including α,β-unsaturated esters, ketones, sulfone, and phosphonate, were successfully converted to the corresponding products **P2**, generally in high yields according to the crude $^1$H NMR analysis (See SI for the full list of acceptor scope).

**Table 1**: 1$^{st}$ Step Reaction Condition Optimization.

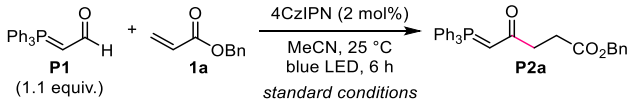


| entry | deviation from standard conditions | **P2a** (%)[a] |
|---|---|---|
| 1 | none | 92 |
| 2 | 3CzClIPN instead of 4CzIPN | 88 |
| 3 | [Ir]-1 instead of 4CzIPN | 9 |
| 4 | [Ir]-2 instead of 4CzIPN | 92 |
| 5 | Me-Acr$^+$ instead of 4CzIPN | N.D. |
| 6 | DMSO instead of MeCN | 49 |
| 7 | $CH_2Cl_2$ instead of MeCN | 55 |
| 8 | acetone instead of MeCN | 86 |
| 9 | without photocatalyst or light | N.D. |
| 10 | with TEMPO (2.0 equiv.) | N.D. |

[a] Yields were determined by $^1$H NMR using 1,1,2,2-tetrachloroethane as an internal standard. N.D. = Not Detected.

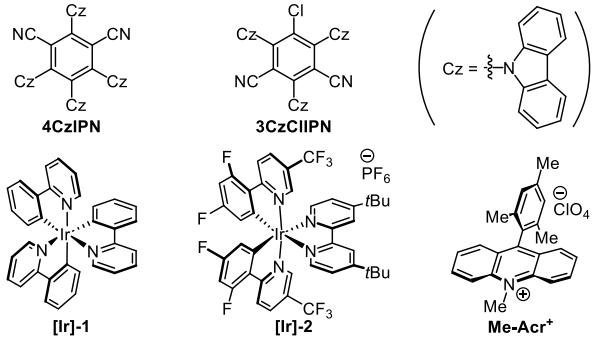

Next, we turned our attention to the 2nd step, where an electrophilic carbon-centered radical is generated from ylide **P2** to react with unactivated alkene fragments.[11] Recently, Miura and Murakami reported a convenient method to generate (alkoxycarbonyl)methyl radicals from ester-stabilized phosphonium ylides based on photoredox catalysis.[15] They used ascorbic acid with these ylides to form the corresponding phosphonium salts, which were subsequently reduced by the highly reducing photoredox catalyst [Ir]-1 (Figure 2a). However, our initial attempt to generate an electrophilic radical from acyl-stabilized ylide **P2'** under identical conditions was unsuccessful, and the reaction with 4-phenyl-1-butene (**2a**) only afforded the desired ketone product **3a** in a low yield (7% NMR yield). Moreover, while a highly reducing photocatalyst would be favorable for this method as the 2nd step, a more oxidizing photocatalyst, such as 4CzIPN, is required at the 1st step. Such a discrepancy in the required photoredox catalyst potentials between each step would be problematic to realize a one-pot sequential process. Therefore, we sought to develop alternative conditions where the same photocatalyst could promote both the 1st and 2nd steps. Specifically, we focused on a method utilizing carbon dioxide radical anion ($CO_2^{\bullet-}$) as a potent single-electron reductant ($E_{1/2}$ = −2.2 V vs. saturated calomel electrode, SCE),[16] which would smoothly reduce a phosphonium salt derived from **P2** to generate the desired electrophilic radical. Given that $CO_2^{\bullet-}$ can be generated from metal formate under photochemical conditions,[17] we envisioned that $CO_2^{\bullet-}$ could be generated from a formate anion or its equivalent as a counteranion of the phosphonium salt, which would be formed in situ from the corresponding Brønsted acid with ylide **P2** (Figure 2b).

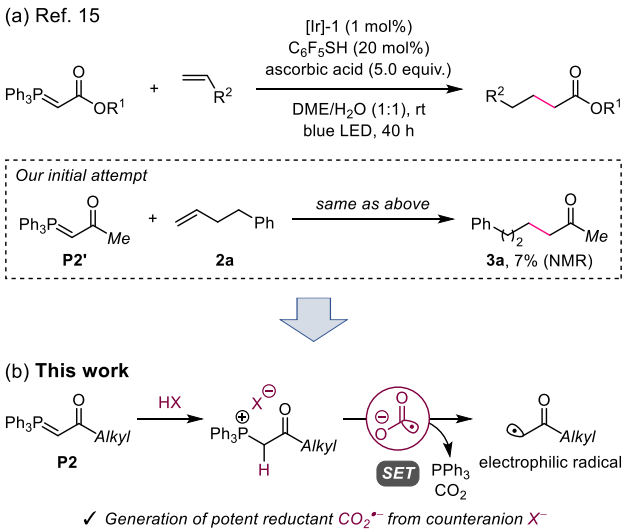


**Figure 2.** Strategy for the generation of electrophilic radical from phosphonium ylide at the 2nd step.

Based on our hypothesis, the effect of acids was investigated for the reaction of ylide **P2'** with **2a** in the presence of 4CzIPN and methyl thiosalicylate (**S1**) as a thiol HAT catalyst under irradiation from a blue light-emitting diode (LED, $\lambda_{max}$ = 448 nm) (Table 2). While the addition of conventional Brønsted acids (Table 2, entries 1–3) or ascorbic acid (Table 2, entry 4) was found to be less effective, the use of formic acid substantially improved the yield of **3a** (Table 2, entry 5), which is consistent with our proposed mechanism (Figure 2b). Further exploration of Brønsted acids acting as a precursor of $CO_2^{\bullet-}$ revealed that oxalic acid dihydrate ($(CO_2H)_2{\cdot}2H_2O$) afforded **3a** in a better yield (Table 2, entry 6). Screening of other parameters identified a mixture of DMSO and $H_2O$ (v/v = 9/1) as a suitable solvent (Table 2, entry 7). Replacing 4CzIPN with [Ir-2], another suitable photocatalyst for the 1st step, was found to be ineffective for the 2nd step (Table 2, entry 8). A prolonged reaction time provided **3a** in a sufficiently high yield (Table 2, entry 9). Control experiments established the necessity of the photocatalyst and light irradiation (Table 2, entry 10).

**Table 2**: 2nd Step Reaction Condition Optimization.

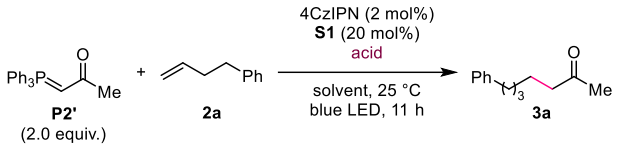


| entry | acid (equiv.) | solvent | **3a** (%)[a] |
|---|---|---|---|
| 1 | $CF_3CO_2H$ (2.0) | DMSO | 19 |
| 2 | $HBF_4$ (2.0) | DMSO | 7 |
| 3 | TsOH (2.0) | DMSO | 4 |
| 4 | ascorbic acid (5.0) | DMSO | N.D. |
| 5 | $HCO_2H$ (5.0) | DMSO | 54 |
| 6 | $(CO_2H)_2{\cdot}2H_2O$ (2.0) | DMSO | 67 |
| 7 | $(CO_2H)_2{\cdot}2H_2O$ (2.0) | DMSO/$H_2O$ (9/1) | 74 |
| 8[b] | $(CO_2H)_2{\cdot}2H_2O$ (2.0) | DMSO/$H_2O$ (9/1) | 21 |
| *9*[c] | *$(CO_2H)_2{\cdot}2H_2O$ (2.0)* | *DMSO/$H_2O$ (9/1)* | *86 (84)* |
| 10[c,d] | $(CO_2H)_2{\cdot}2H_2O$ (2.0) | DMSO/$H_2O$ (9/1) | trace |

[a] Yields were determined by $^1$H NMR using 1,1,2,2-tetrachloroethane as an internal standard. The isolated yield is shown in parentheses. [b] [Ir-2] was used instead of 4CzIPN. [c] Reaction time was 20 h. [d] No light or photocatalyst.

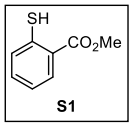


**Mechanistic Investigations.** To better understand the reaction mechanism, we carried out a series of analytical and experimental studies for the 1st and 2nd steps (Figure 3, see SI for details). Stern–Volmer fluorescence quenching studies for the 1st step revealed that **P1** quenches the excited state of 4CzIPN more efficiently than does acceptor **1a** (Figure 3, 1A). In addition, electrochemical analysis of **P1** indicated its oxidation potential as 0.96 V vs. SCE (Figure 3, 1B), which is lower than the reduction potential of the excited state of 4CzIPN ($E(PC^*/PC^{\bullet-})$ = 1.35 V vs. SCE).[18] Hence, the reaction proceeds with the single-electron oxidation of the phosphonium ylide via a reductive quenching cycle to generate radical cation **I** (Figure 3, 1C).[19] At this point, we reasoned that two electron-withdrawing groups of **I**, a carbonyl moiety and a quaternary phosphonium moiety, would render the neighboring carbon radical center highly electrophilic, which could act as a HAT mediator to abstract a hydrogen atom from the formyl C–H bond of **P1** to generate the nucleophilic acyl radical **II**.[10] The bond dissociation free energies (BDFEs) of acidic C–H bonds in the conjugate acids

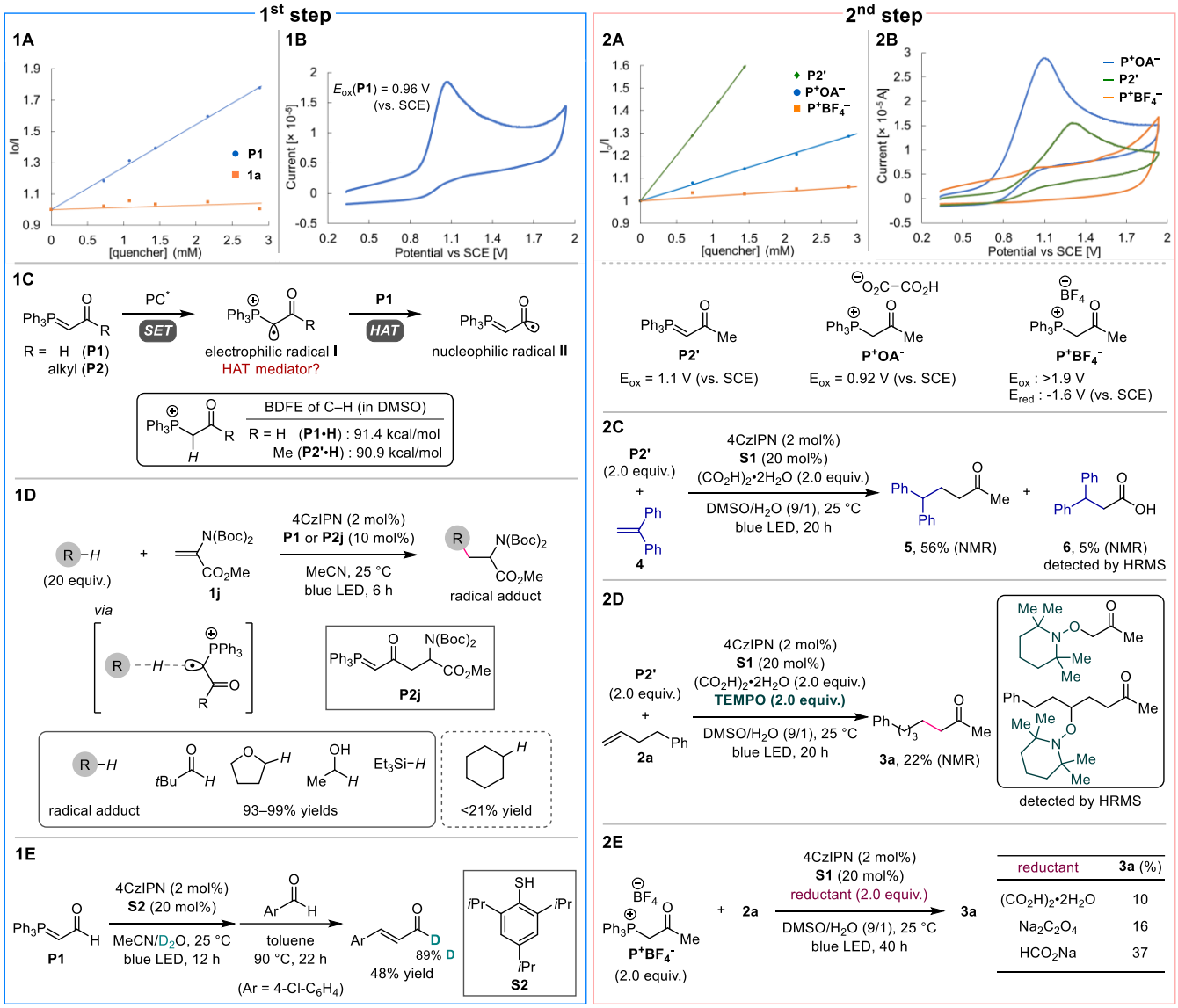


**Figure 3.** Mechanistic investigations for the 1st step (left) and the 2nd step (right). (1A) Stern–Volmer quenching studies for the 1st step. (1B) Cyclic voltammogram of **P1**. (1C) Possible mechanism for generation of acyl radical **II**. (1D) Evaluation of the HAT ability of phosphonium ylides. (1E) Photocatalytic H/D exchange of **P1**. (2A) Stern–Volmer quenching studies for the 2nd step. (2B) Comparison of redox potential of phosphonium species. (2C) Radical-trapping experiment with **4**. (2D) Radical-trapping experiment with TEMPO. (2E) Importance of ion-pair formation.

of phosphonium ylides (**P1·H** and **P2'·H**) in DMSO are estimated to be 91.4 and 90.9 kcal/mol, respectively.[20,21] These values indicate that the formyl-stabilized ylide and the acyl-stabilized ylide have a similar reactivity in the hydrogen-atom abstraction process. To obtain more evidence for the HAT ability of electrophilic radical **I**, the parent phosphonium ylides were subjected to the conditions for photoinduced alkylation of C–H or Si–H bonds using **1j** as a radical acceptor (Figure 3, 1D).[22] The use of a catalytic amount of phosphonium ylide **P1** or **P2j** was found to promote the reactions with several substrates commonly used in HAT catalysis, affording the corresponding radical adducts to **1j** in high yields except for cyclohexane, which bears relatively strong C–H bonds. These results support that the electrophilic radical **I** is a good HAT mediator for the 1st step of our method. We also conducted the photocatalytic H/D exchange of the formyl C–H bond in **P1** (Figure 3, 1E). The reaction of **P1** in the presence of 4CzIPN and thiol catalyst **S2** in a mixed solvent of MeCN and $D_2O$ under visible-light irradiation, followed by the Wittig reaction with 4-chlorobenzaldehyde, afforded deuterated 4-chlorocinnamaldehyde. A high deuterium incorporation (89% D) at the formyl group of the product is consistent with the previously reported mechanism, which includes the generation of a nucleophilic acyl radical and the subsequent C–D bond formation via the deuterium-atom transfer from a deuterated thiol catalyst.[23]

Next, to characterize the radical precursor responsible for the 2nd step, we performed Stern–Volmer fluorescence quenching studies and electrochemical analysis of ylide **P2'** and the related phosphonium salts (Figure 3, 2A and 2B). The Stern–Volmer plots showed that the quenching rate of phosphonium oxalate (**P⁺OA⁻**), which was prepared by

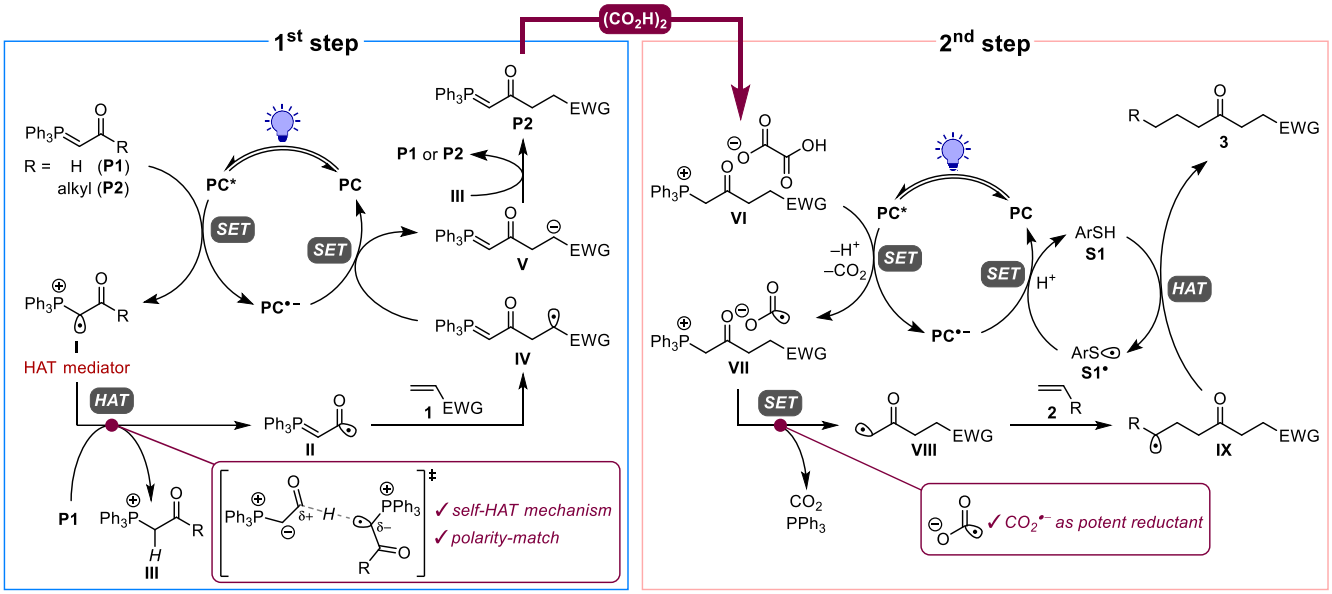


**Figure 4**. Proposed mechanism for sequential photocatalysis.

mixing an equimolar amount of **P2'** with oxalic acid, was different from those of **P2'** and phosphonium tetrafluoroborate (**P⁺BF₄⁻**). Notably, **P⁺OA⁻** quenched the excited state of 4CzIPN dramatically more than did **P⁺BF₄⁻**, indicating a non-innocent role of the counteranion in **P⁺OA⁻**. The cyclic voltammetry reflected different redox behaviors of these species (Figure 3, 2B). While **P2'** and **P⁺OA⁻** had an oxidation potential at 1.1 V vs. SCE and 0.92 V vs. SCE, respectively, **P⁺BF₄⁻** did not show any obvious oxidation peak within the measurement range. Instead, the reduction potential of **P⁺BF₄⁻** was found to be −1.6 V vs. SCE. Given the redox potential of 4CzIPN ($E$(PC*/PC•⁻) = 1.35 V vs. SCE; $E$(PC/PC•⁻) = −1.21 V vs. SCE),[18] these observations explain the experimental outcome: the use of a conventional acid such as $HBF_4$ resulted in a low yield of **3a** due to a thermodynamically unfavorable SET between 4CzIPN and the corresponding phosphonium salt **P⁺BF₄⁻** (Table 2, entry 2). On the other hand, the use of $(CO_2H)_2{\cdot}2H_2O$ was effective because the resulting phosphonium oxalate **P⁺OA⁻** could be oxidized by 4CzIPN to generate the potent reductant $CO_2^{\bullet-}$ via the decomposition of the oxalate radical anion (Table 2, entry 6).[24] Thus, we next sought to obtain evidence for the generation of $CO_2^{\bullet-}$ by capturing it with 1,1-diphenylethylene (**4**) as a radical-trapping agent (Figure 3, 2C). Indeed, after a reaction of **P2'** with **4** under optimal conditions, the expected radical adduct **6** was detected by $^1$H NMR analysis and high-resolution mass spectrometry (HRMS), along with **5** as the major product. Furthermore, another radical-trapping experiment using TEMPO suppressed the formation of ketone product **3a**, and two kinds of TEMPO adducts were detected by HRMS, indicating the generation of an acetyl-substituted carbon-centered radical and the subsequent radical addition to alkene **2a** (Figure 3, 2D). Lastly, to confirm the effect of the formation of an ion pair comprising a phosphonium and an oxalate, phosphonium salt **P⁺BF₄⁻** was subjected to conditions for the 2nd step using several $CO_2^{\bullet-}$ precursors (Figure 3, 2E). Among oxalic acid, oxalate salt, and formate salt, none of them showed comparable results to the optimized conditions, indicating that the formation of the ion pair via a thermodynamically favorable acid-base reaction between phosphonium ylide **P2'** and oxalic acid contributes to the efficient single-electron reduction of the phosphonium salt.

Taken together, we propose the mechanism shown in Figure 4. For the 1st step, the single-electron oxidation of ylide **P1** (or **P2** after the first catalytic cycle) by the excited state of 4CzIPN (**PC***) generates highly electrophilic radical **I**, which can act as a HAT mediator as demonstrated in Figure 3, 1D. Here, the negative charge at the ylide α-carbon of **P1** renders its formyl C–H bond highly hydridic. Therefore, the HAT between **I** and **P1** takes place selectively due to the favorable polar effect,[25] and acyl radical **II** is efficiently generated along with phosphonium salt **III**. Since **II** has a nucleophilic character, it undergoes Giese-type addition to Michael acceptor **1** to afford intermediate **IV**. The subsequent SET by the reduced form of photocatalyst (**PC•⁻**) converts **IV** to **V**, which deprotonates a moderately acidic α-C–H bond of **III** to furnish the intermediate ylide **P2**. After **P1** is completely converted to **P2** in the 1st step, oxalic acid is added to the system to form phosphonium oxalate **VI**, which engages in the catalytic cycle of the 2nd step. As discussed in 2A and 2B of Figure 3, **VI** can be oxidized by the same photocatalyst used in the 1st step. Upon deprotonation and decarboxylation, $CO_2^{\bullet-}$ is generated as a potent reductant, which facilitates the cleavage of a C–P bond in the phosphonium moiety of the same ion pair **VII** to yield electrophilic radical **VIII**. The addition of **VIII** to unactivated alkene **2** provides carbon-centered radical **IX**, which accepts a hydrogen atom from thiol catalyst **S1** to afford the desired product **3**. Finally, the resulting thiyl radical **S1•** is reduced by **PC•⁻** with the concomitant protonation, closing the catalytic cycle of the 2nd step. The observed quantum yield ($\Phi$) value was much lower than 1 for each step ($\Phi$ = 6.3 × 10$^{-2}$ for the 1st step and 3.0 × 10$^{-3}$ for the 2nd step. See SI for details), which supports closed photocatalytic cycles and thus the mechanism of sequential photocatalysis.

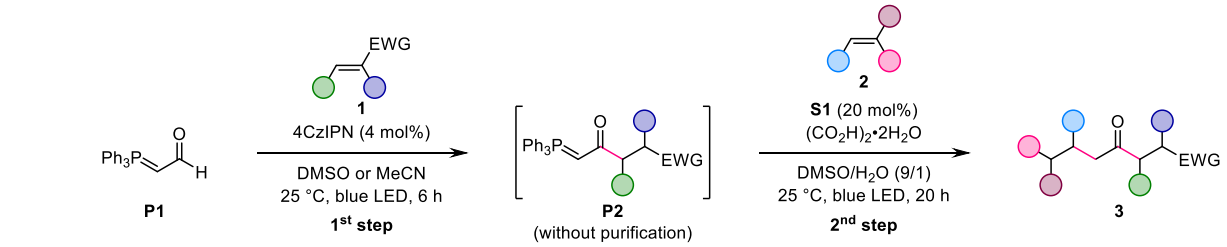


## *Michael Acceptors* [a]

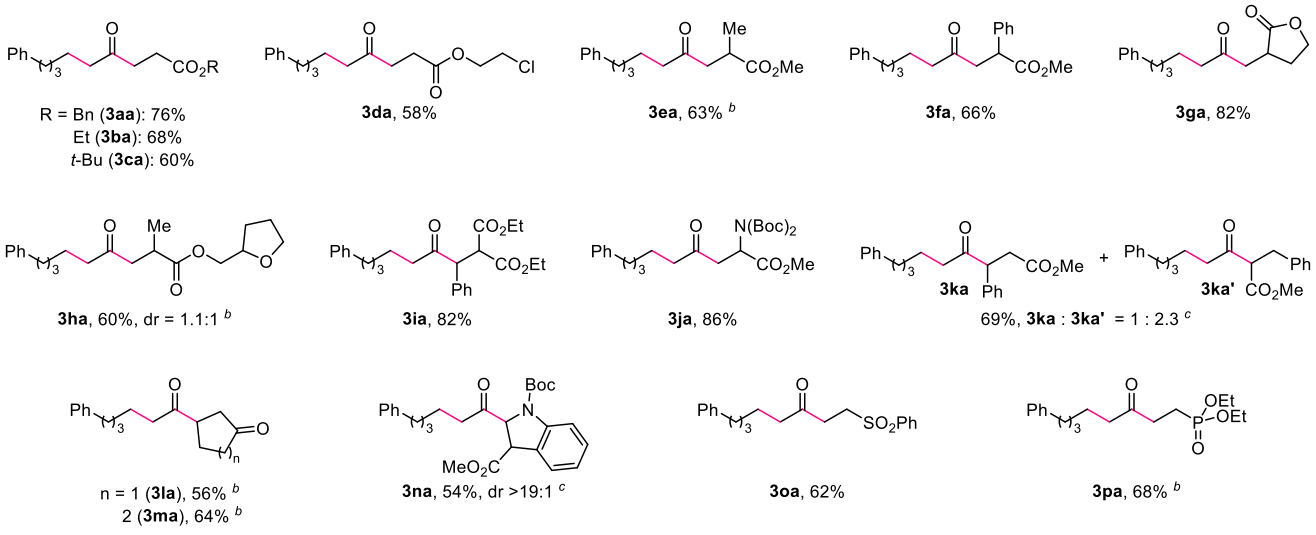


## *Alkenes* [d]

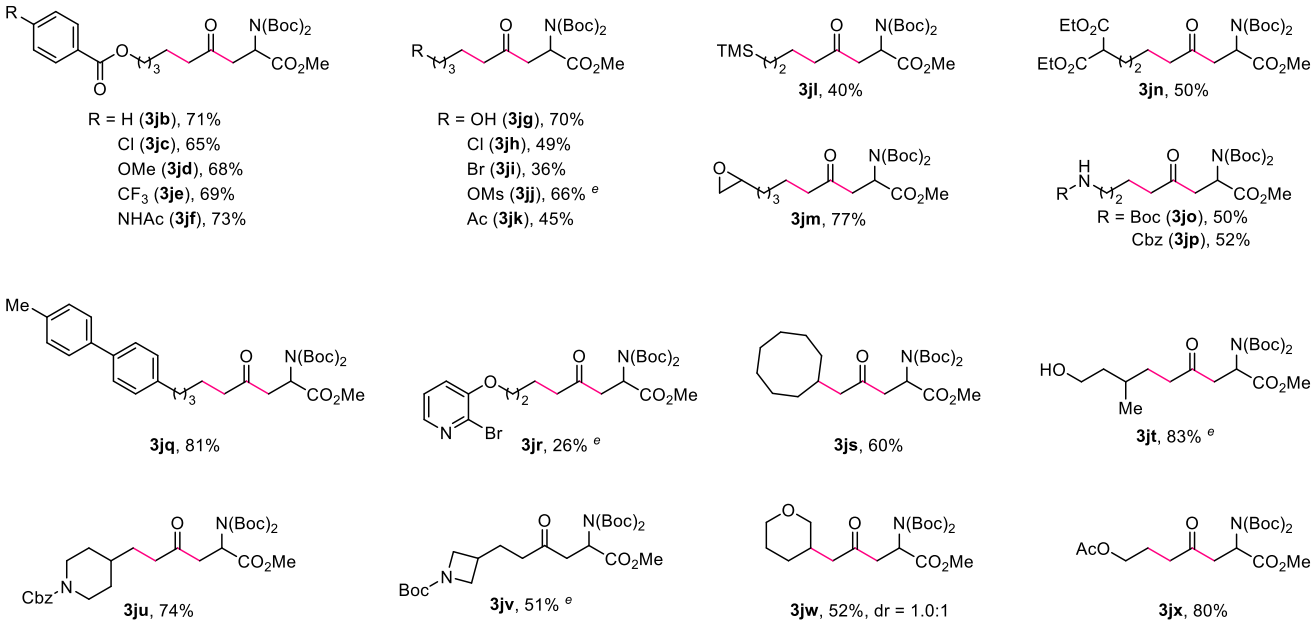


**Figure 5**. Substrate scope for sequential photocatalysis. Reaction conditions: [1st step] **P1** (0.44 mmol), **1** (0.40 mmol), and 4CzIPN (0.0080 mmol) in MeCN or DMSO, blue LED ($\lambda_{max}$ = 448 nm), 25 °C, 6 h; [2nd step] **P2** (not isolated), **2** (0.20 mmol), $(CO_2H)_2 \cdot 2H_2O$ (0.40 mmol), and methyl thiosalicylate (**S1**, 0.040 mmol) in DMSO/$H_2O$ (9/1), blue LED ($\lambda_{max}$ = 448 nm), 25 °C, 20 h. Isolated yields over 2 steps are shown. See SI for full experimental details. [a] MeCN (4.0 mL) was used as a solvent for the 1st step. [b] $LiBF_4$ (0.080 mmol) was added for the 1st step. [c] Regioisomeric ratio and diastereomer ratio (dr) were determined by $^1H$ NMR of the crude product. [d] DMSO (2.0 mL) was used as a solvent for the 1st step. [e] Reaction time for the 2nd step was 40 h.

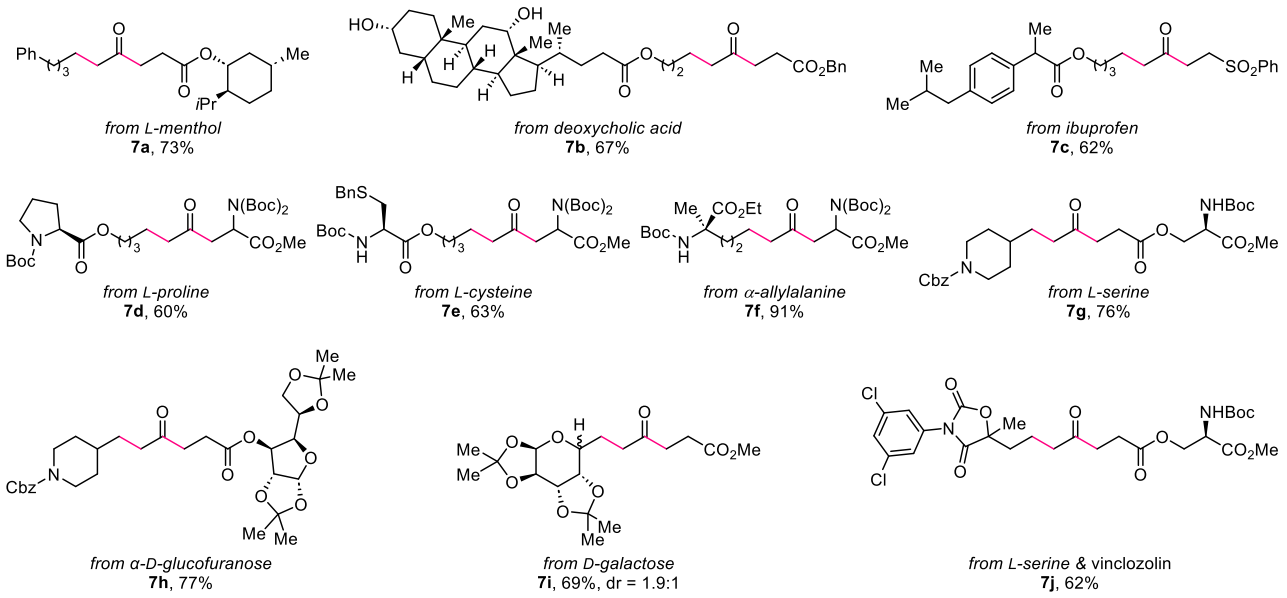


**Figure 6**. Radical linchpin coupling with biorelevant molecules. See SI for full experimental details.

**Development of Sequential Process.** Based on the optimized conditions for each step together with the proposed mechanism, we sought to develop a one-pot protocol for sequential photocatalysis using ambiphilic radical linchpin **P1** with two alkene fragments (**1** and **2**) to access unsymmetrical ketone product **3** (Figure 5). Gratifyingly, reaction conditions established for each step were successfully combined to realize the sequential process, and intermediate ylide **P2** formed after the 1st step could be directly used for the 2nd step without purification (see SI for detailed protocols). Of note, the photocatalyst added before the 1st step was still active in the 2nd step, establishing a unique protocol for the sequential process where a single photocatalyst promotes two mechanistically distinct radical reactions successively in one pot. With the optimized experimental protocols in hand, we sought to evaluate the scope of the sequential photocatalysis. Firstly, various Michael acceptors **1** were employed for the 1st step of our method to unite them with **P1** and **2a**, affording 1,4-dicarbonyl compounds in most cases. Acrylate derivatives were well tolerated to give the desired γ-oxoesters **3aa**–**3ka** in moderate to good yields. In the case of acceptors with insufficient reactivity in the 1st step, the addition of a catalytic amount of $LiBF_4$ was effective, providing acceptable yields of the products. Highly activated alkenes furnished the corresponding products **3ia**–**3ja** in high yields. When methyl cinnamate was used, a mixture of two regioisomers, **3ka** and **3ka'**, was obtained. Various types of electron-deficient alkenes, such as an activated indole derivative, vinyl sulfone, vinyl phosphonate, and α,β-unsaturated cyclic ketones, were also applicable to the present method, affording structurally diverse dialkyl ketones **3la**–**3pa**.

We then turned our attention to the scope of unactivated or electron-rich alkenes **2** as partners in the 2nd step. Dehydroalanine derivative **1j** was used as a suitable alkene for the 1st step of these reactions, affording α-monosubstituted amino acid derivatives containing various functionalities as the final products. 3-Butenyl benzoate derivatives with a range of substituents at the *para* position of the phenyl group provided the corresponding products **3jb**–**3jf** in good yields. Terminal alkenes bearing reactive functional groups, such as hydroxy, (pseudo)halogen, acetyl, silyl, and epoxy groups, were well tolerated (**3jg**–**3jm**). In addition, the relatively acidic C–H bond of a malonate moiety and the N–H bonds of protected amino groups were also successfully incorporated into the products (**3jn**–**3jp**). These examples display the high functional group tolerance of our method. On the other hand, an alkene with a basic pyridine moiety showed a decreased reactivity, probably due to the interference with the formation of phosphonium oxalate (**3jr**). Besides monosubstituted alkenes, a cyclic alkene and α,α-disubstituted alkenes were also compatible with this method, furnishing the desired products **3js**–**3jv** in moderate to good yields. The reactions with enol ethers as electron-rich alkenes proceeded well to afford the corresponding products **3jw**–**3jx**.

Encouraged by the broad scope of alkenes for both steps, we conducted the radical linchpin coupling with complex alkene fragments derived from biorelevant molecules (Figure 6). The derivatives of naturally occurring bioactive compounds, such as L-menthol and deoxycholic acid, and ibuprofen as a representative pharmaceutical, were successfully employed for the sequential photocatalysis (**7a**–**7c**). Natural and unnatural amino acids, including L-proline, L-cysteine, α-allylalanine, and L-serine, could be incorporated to afford the desired 1,4-dicarbonyl products in moderate to high yields (**7d**–**7g**). The same protocol was also applicable to acetonide-protected sugar derivatives (**7h**–**7i**). Finally, two kinds of biorelevant compounds, L-serine, and vinclozolin, could be connected to furnish the product **7j** in one pot, demonstrating the utility of our method as a tool for the rapid connection of two complex molecules.

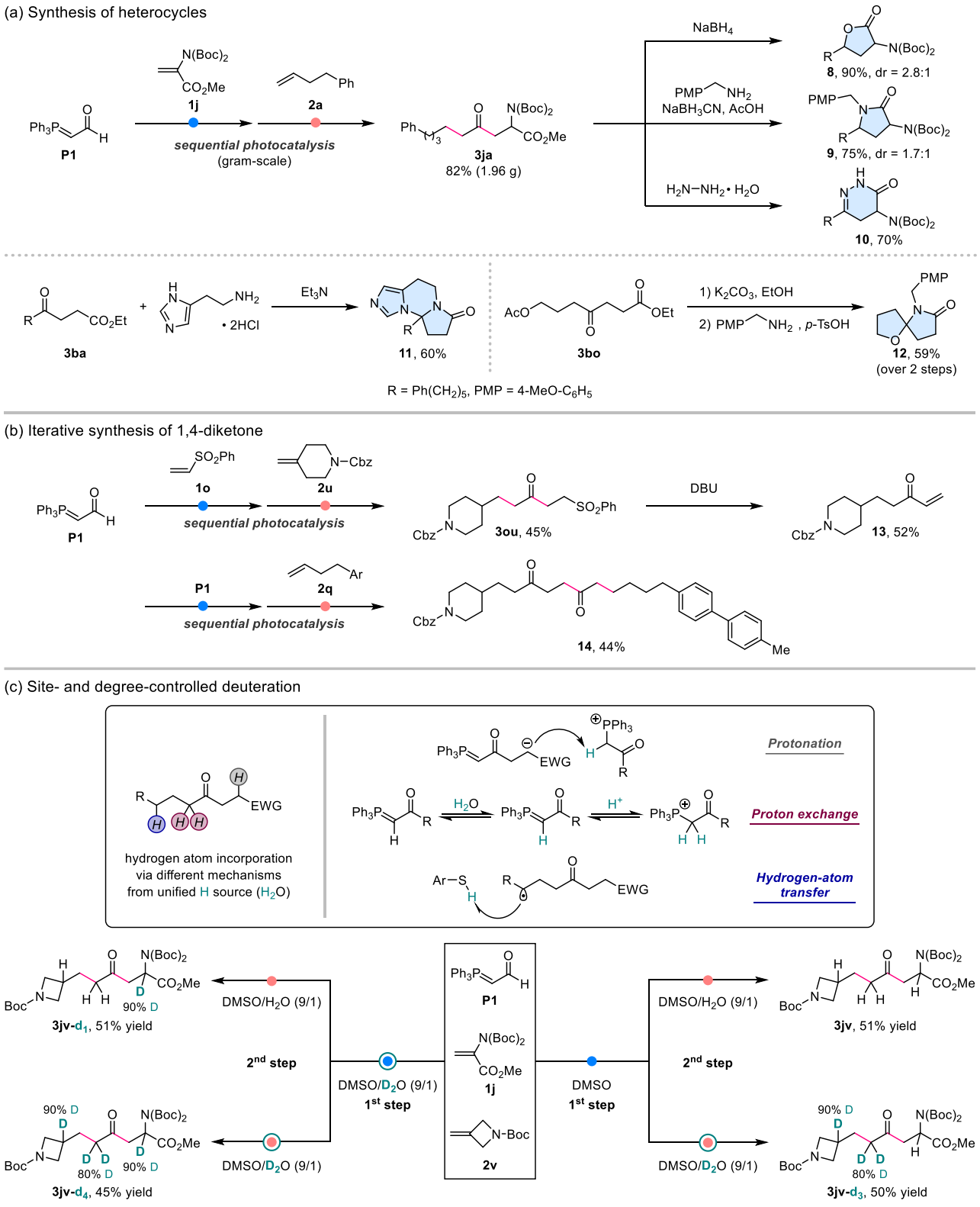


**Figure 7**. Synthetic applications. See SI for details.

Taking advantage of the versatility of products, several synthetic applications of the sequential photocatalysis were carried out (Figure 7). Firstly, as 1,4-dicarbonyls can be transformed into a diverse array of structures by making use of their two carbonyl moieties, the obtained products were derivatized to access various heterocycles (Figure 7a). As a model product, γ-oxoester **3ja** was synthesized on a gram scale. Transformations of the ketone moiety of **3ja**, such as reduction, reductive amination, and condensation, gave rise to a new oxygen or nitrogen nucleophile, which subsequently reacted with the terminal ester group to form cyclized products **8**–**10** in good to high yields. The reaction of γ-oxoester **3ba** with histamine as a bis-nucleophile produced fused triazaheterocycle **11**, which is a synthetic

congener of glochidine.[26] Furthermore, the deacetylation of the terminal acetoxy group of **3bo**, followed by a tandem imine formation/aminoacetalyzation/amidation sequence, afforded spirocyclic aminoacetal **12** in 2 steps. Next, our protocol was applied to an iterative strategy for the synthesis of a 1,4-diketone (Figure 7b). The sequential photocatalysis using **P1**, **1o**, and **2u** under the optimal conditions provided the corresponding β-sulfonyl ketone **3ou**, which was converted to α,β-unsaturated ketone **13** by a base-promoted β-elimination of the sulfonyl group. Repeating the sequential process to assemble **13** with linchpin **P1** and another alkene **2q** successfully proceeded to afford the desired 1,4-diketone **14**. This approach potentially expands the scope of accessible 1,4-dicarbonyl products using our method. Lastly, we sought to synthesize a series of deuterated isotopomers of the product in a site- and degree-controlled manner, which was enabled by the unique mechanism of the present method (Figure 7c). Specifically, three kinds of C–H bonds in the target structure were formed during the sequential process via different mechanisms for incorporation of a hydrogen atom: protonation of a carbanion adjacent to the electron-withdrawing group, reversible proton exchange at the ylide-derived α-carbon, and hydrogen-atom transfer from a thiol catalyst to a carbon-centered radical derived from an unactivated alkene. Notably, $H_2O$ can serve as a unified hydrogen source for these mechanisms. Therefore, we modified the protocol for the sequential process, where a readily available deuterium source, $D_2O$, was added or replaced with $H_2O$ at each step according to the desired degree of deuteration of the product. While non-deuterated product **3jv** was obtained in 51% yield under the optimal conditions using **P1**, **1j**, and **2v**, the use of a mixture of DMSO and $D_2O$ (v/v = 9/1) only at the 1st step afforded mono-deuterated product **3jv-d$_1$** without affecting the product yield. Moreover, replacing $H_2O$ with $D_2O$ at the 2nd step provided tri-deuterated product **3jv-d$_3$**, and the use of DMSO/$D_2O$ cosolvent at both steps furnished tetra-deuterated product **3jv-d$_4$** as the major product. These results demonstrate that our method is useful for preparing selectively deuterated molecules.[27]

## Conclusions

In summary, a sequential photocatalysis involving two mechanistically distinct radical additions has been developed. This process is enabled by multiple roles of ambiphilic radical linchpin **P1**, which serves as a nucleophilic and an electrophilic carbon-centered radical source, as well as a HAT mediator, in the presence of a single photoredox catalyst. Various alkene fragments, such as those with functional groups that would be reactive in a polar mechanism and complex biorelevant molecules, can be used in the bidirectional formation of two C–C bonds from **P1** in one pot. Overall, the present radical linchpin coupling strategy has enabled a rapid and modular access to synthetically valuable 1,4-dicarbonyl compounds. Further investigations on the radical reactivity of phosphonium ylides, especially as a novel HAT catalyst platform, are currently underway in our laboratory.

# ASSOCIATED CONTENT

## Supporting Information

The Supporting Information is available free of charge at http://pubs.acs.org.

Experimental procedures, mechanistic studies, compound characterization data, and NMR spectra (PDF)

# AUTHOR INFORMATION


## Corresponding Author

**Akira Matsumoto** – *Graduate School of Pharmaceutical Sciences, Kyoto University, Sakyo, Kyoto 606-8501, Japan*; orcid.org/0000-0002-3719-8597; Email: matsumoto.akira.3c@kyoto-u.ac.jp

**Keiji Maruoka** – *Graduate School of Pharmaceutical Sciences, Kyoto University, Sakyo, Kyoto 606-8501, Japan; School of Chemical Engineering and Light Industry, Guangdong University of Technology, Guangzhou 510006, China*; orcid.org/0000-0002-0044-6411; Email: maruoka.keiji.4w@kyoto-u.ac.jp

## Author

**Natsumi Maeda** – *Graduate School of Pharmaceutical Sciences, Kyoto University, Sakyo, Kyoto 606-8501, Japan*; orcid.org/0000-0002-8080-138X.


## Notes

The authors declare no competing financial interest.

# ACKNOWLEDGMENT


K.M. gratefully acknowledges financial support via KAKENHI grants No. 21H05026 and 23H04910. A.M. is thankful for financial support via JSPS KAKENHI grant No. 22K14680. The authors thank Kishida chemical Co., Ltd. for donation of (*R*)-*N*-Boc-α-allylalanine ethyl ester (starting material of **7f**).


# REFERENCES


(1) (a) Herrera, R. P.; Marqués-López, E. *Multicomponent Reactions: Concepts and Applications for Design and Synthesis*; Wiley: New York, 2015 (b) Zhi, S.; Ma, X.; Zhang, W. Consecutive Multicomponent Reactions for the Synthesis of Complex Molecules. *Org. Biomol. Chem.* **2019**, *17*, 7632–7650. (c) Dömling, A.; Wang, W.; Wang, K. Chemistry and Biology of Multicomponent Reactions. *Chem. Rev.* **2012**, *112*, 3083–3135. (d) Ruijter, E.; Scheffelaar, R.; Orru, R. V. A. Multicomponent Reaction Design in the Quest for Molecular Complexity and Diversity. *Angew. Chem., Int. Ed.* **2011**, *50*, 6234–6246. (e) Touré, B. B.; Hall, D. G. Natural Product Synthesis Using Multicomponent Reaction Strategies. *Chem. Rev.* **2009**, *109*, 4439–4486.

(2) (a) Smith, A. B., III; Boldi, A. M. Multicomponent Linchpin Couplings of Silyl Dithianes via Solvent-Controlled Brook Rearrangement. *J. Am. Chem. Soc.* **1997**, *119*, 6925–6926. (b) Smith, A. B., III; Pitram, S. M.; Boldi, A. M.; Gaunt, M. J.; Sfouggatakis, C.; Moser, W. H. Multicomponent Linchpin Couplings. Reaction of Dithiane Anions with Terminal Epoxides, Epichlorohydrin, and Vinyl Epoxides: Efficient, Rapid, and Stereocontrolled Assembly of Advanced Fragments for Complex Molecule Synthesis. *J. Am. Chem. Soc.* **2003**, *125*, 14435–14445. (c) Nicewicz, D. A.; Johnson, J. S. Three-Component Coupling Reactions of Silylglyoxylates, Alkynes, and Aldehydes: A Chemoselective One-Step Glycolate Aldol Construction. *J. Am. Chem. Soc.* **2005**, *127*, 6170–6171. (d) Heller, S. T.; Newton, J. N.; Fu, T.; Sarpong, R. One-Pot Unsymmetrical Ketone Synthesis Employing a Pyrrole-Bearing Formal Carbonyl Dication Linchpin Reagent. *Angew. Chem., Int. Ed.* **2015**, *54*, 9839–9843. (e) Murray, S. A.; Liang, M. Z.; Meek, S. J. Stereoselective Tandem Bis-Electrophile Couplings of Diborylmethane. *J. Am. Chem. Soc.* **2017**, *139*, 14061–14064. (f) Zhang, L.; Lovinger, G. J.; Edelstein, E. K.; Szymaniak, A. A.; Chierchia, M. P.; Morken, J. P. Catalytic Conjunctive

Cross-Coupling Enabled by Metal-Induced Metallate Rearrangement. *Science* **2016**, *351*, 70–74. (g) Hurst, T. E.; Deichert, J. A.; Kapeniak, L.; Lee, R.; Harris, J.; Jessop, P. G.; Snieckus, V. Sodium Methyl Carbonate as an Effective C1 Synthon. Synthesis of Carboxylic Acids, Benzophenones, and Unsymmetrical Ketones. *Org. Lett.* **2019**, *21*, 3882–3885.

(3) (a) Deng, Y.; Smith, A. B., III. Evolution of Anion Relay Chemistry: Construction of Architecturally Complex Natural Products. *Acc. Chem. Res.* **2020**, *53*, 988–1000. (b) Boyce, G. R.; Greszler, S. N.; Johnson, J. S.; Linghu, X.; Malinowski, J. T.; Nicewicz, D. A.; Satterfield, A. D.; Schmitt, D. C.; Steward, K. M. Silyl Glyoxylates. Conception and Realization of Flexible Conjunctive Reagents for Multicomponent Coupling. *J. Org. Chem.* **2012**, *77*, 4503–4515.

(4) (a) Yan, M.; Lo, J. C.; Edwards, J. T.; Baran, P. S. Radicals: Reactive Intermediates with Translational Potential. *J. Am. Chem. Soc.* **2016**, *138*, 12692–12714. (b) Studer, A.; Curran, D. P. Catalysis of Radical Reactions: A Radical Chemistry Perspective. *Angew. Chem., Int. Ed.* **2016**, *55*, 58–102. (c) Romero, K. J.; Galliher, M. S.; Pratt, D. A.; Stephenson, C. R. J. Radicals in Natural Product Synthesis. *Chem. Soc. Rev.* **2018**, *47*, 7851–7866.

(5) (a) Shaw, M. H.; Twilton, J.; MacMillan, D. W. C. Photoredox Catalysis in Organic Chemistry. *J. Org. Chem.* **2016**, *81*, 6898–6926. (b) Romero, N. A.; Nicewicz, D. A. Organic Photoredox Catalysis. *Chem. Rev.* **2016**, *116*, 10075–10166. (c) McAtee, R. C.; McClain, E. J.; Stephenson, C. R. J. Illuminating Photoredox Catalysis. *Trends Chem.* **2019**, *1*, 111–125.

(6) Novaes, L. F. T.; Liu, J.; Shen, Y.; Lu, L.; Meinhardt, J. M.; Lin, S. Electrocatalysis as an Enabling Technology for Organic Synthesis. *Chem. Soc. Rev.* **2021**, *50*, 7941–8002.

(7) (a) Yang, B.; Lu, S.; Wang, Y.; Zhu, S. Diverse Synthesis of C2-Linked Functionalized Molecules via Molecular Glue Strategy with Acetylene. *Nat. Commun.* **2022**, *13*, 1858. (b) Kim, S.; Yoon, J.-Y. Free Radical-Mediated Ketone Synthesis from Alkyl Iodides via Sequential Radical Acylation Approach. *J. Am. Chem. Soc.* **1997**, *119*, 5982–5983. (c) Anthore-Dalion, L.; Liu, Q.; Zard, S. Z. A Radical Bidirectional Fragment Coupling Route to Unsymmetrical Ketones. *J. Am. Chem. Soc.* **2016**, *138*, 8404–8407.

(8) (a) Trost, B. M.; Hung, C.-I.; Saget, T.; Gnanamani, E. Branched Aldehydes as Linchpins for the Enantioselective and Stereodivergent Synthesis of 1,3-Aminoalcohols Featuring a Quaternary Stereocentre. *Nature Catalysis* **2018**, *1*, 523–530. (b) Hayashi, Y.; Saitoh, T.; Arase, H.; Kawauchi, G.; Takeda, N.; Shimasaki, Y.; Sato, I. Two-Pot Synthesis of Chiral 1,3-*syn*-Diols through Asymmetric Organocatalytic Aldol and Wittig Reactions Followed by Domino Hemiacetal/Oxy-Michael Reactions. *Chem.—Eur. J.* **2018**, *24*, 4909–4915.

(9) Banerjee, A.; Lei, Z.; Ngai, M.-Y. Acyl Radical Chemistry via Visible-Light Photoredox Catalysis. *Synthesis* **2019**, *51*, 303–333.

(10) For recent reviews on photoinduced Hydrogen-atom transfer: (a) Cao, H.; Tang, X.; Tang, H.; Yuan, Y.; Wu, J. Photoinduced Intermolecular Hydrogen Atom Transfer Reactions in Organic Synthesis. *Chem Catalysis* **2021**, *1*, 523–598. (b) Capaldo, L.; Ravelli, D.; Fagnoni, M. Direct Photocatalyzed Hydrogen Atom Transfer (HAT) for Aliphatic C–H Bonds Elaboration. *Chem. Rev.* **2022**, *122*, 1875–1924. (c) Capaldo, L.; Quadri, L. L.; Ravelli, D. Photocatalytic Hydrogen Atom Transfer: The Philosopher's Stone for Late-Stage Functionalization? *Green Chem.* **2020**, *22*, 3376–3396.

(11) (a) Lenardon, G. V. A.; Nicchio, L.; Fagnoni, M. Photogenerated Electrophilic Radicals for the Umpolung of Enolate Chemistry. *J. Photochem. Photobiol. C* **2021**, *46*, 100387. (b) Lee, K. N.; Ngai, M. Y. Recent Developments in Transition-Metal Photoredox-Catalysed Reactions of Carbonyl Derivatives. *Chem. Commun.* **2017**, *53*, 13093–13112.

(12) Mečiarová, M.; Tisovský, P.; Šebesta, R. Enantioselective Organocatalysis Using SOMO Activation. *New J. Chem.* **2016**, *40*, 4855–4864.

(13) Lemmerer, M.; Schupp, M.; Kaiser, D.; Maulide, N. Synthetic Approaches to 1,4-Dicarbonyl Compounds. *Nat. Synth.* **2022**, *1*, 923–935.

(14) Rohe, S.; Morris, A. O.; McCallum, T.; Barriault, L. Hydrogen Atom Transfer Reactions via Photoredox Catalyzed Chlorine Atom Generation. *Angew. Chem., Int. Ed.* **2018**, *57*, 15664–15669.

(15) Miura, T.; Funakoshi, Y.; Nakahashi, J.; Moriyama, D.; Murakami, M. Synthesis of Elongated Esters from Alkenes. *Angew. Chem., Int. Ed.* **2018**, *57*, 15455–15459.

(16) Lamy, E.; Nadjo, L.; Saveant, J. M. Standard Potential and Kinetic Parameters of the Electrochemical Reduction of Carbon Dioxide in Dimethylformamide. *J. Electroanal. Chem.* **1977**, *78*, 403–407.

(17) For selected examples: (a) Huang, Y.; Hou, J.; Zhan, L.-W.; Zhang, Q.; Tang, W.-Y.; Li, B.-D. Photoredox Activation of Formate Salts: Hydrocarboxylation of Alkenes via Carboxyl Group Transfer. *ACS Catal.* **2021**, *11*, 15004–15012. (b) Alektiar, S. N.; Wickens, Z. K. Photoinduced Hydrocarboxylation via Thiol-Catalyzed Delivery of Formate Across Activated Alkenes. *J. Am. Chem. Soc.* **2021**, *143*, 13022–13028. (c) Chmiel, A. F.; Williams, O. P.; Chernowsky, C. P.; Yeung, C. S.; Wickens, Z. K. Non-Innocent Radical Ion Intermediates in Photoredox Catalysis: Parallel Reduction Modes Enable Coupling of Diverse Aryl Chlorides. *J. Am. Chem. Soc.* **2021**, *143*, 10882–10889. (d) Hendy, C. M.; Smith, G. C.; Xu, Z.; Lian, T.; Jui, N. T. Radical Chain Reduction via Carbon Dioxide Radical Anion ($CO_2^{\bullet-}$). *J. Am. Chem. Soc.* **2021**, *143*, 8987–8992. (e) Wang, H.; Gao, Y.; Zhou, C.; Li, G. Visible-Light-Driven Reductive Carboarylation of Styrenes with $CO_2$ and Aryl Halides. *J. Am. Chem. Soc.* **2020**, *142*, 8122–8129.

(18) Luo, J.; Zhang, J. Donor–Acceptor Fluorophores for Visible-Light-Promoted Organic Synthesis: Photoredox/Ni Dual Catalytic $C(sp^3)$–$C(sp^2)$ Cross-Coupling. *ACS Catal.* **2016**, *6*, 873–877.

(19) The related radical species was proposed in recent reports. (a) Das, M.; Vu, M. D.; Zhang, Q.; Liu, X.-W. Metal-Free Visible Light Photoredox Enables Generation of Carbyne Equivalents via Phosphonium Ylide C-H Activation. *Chem. Sci.* **2019**, *10*, 1687–1691. (b) Duy Vu, M.; Leng, W.-L.; Hsu, H.-C.; Liu, X.-W. Alkene Synthesis Using Phosphonium Ylides as Umpolung Reagents. *Asian J. Org. Chem.* **2019**, *8*, 93–96. (c) Wang, M.; He, Y.-Q.; Zhu, Y.; Song, Z.-B.; Wang, X.-Y.; Huang, H.-Y.; Cao, B.-P.; Tian, W.-F.; Xiao, Q. The Wavelength-Regulated Stereodivergent Synthesis of (*Z*)- and (*E*)-1,4-Enediones from Phosphonium Ylides. *Org. Chem. Front.* **2021**, *8*, 5934–5940.

(20) (a) Zhang, X. M.; Bordwell, F. G. Equilibrium Acidities and Homolytic Bond Dissociation Energies of the Acidic Carbon-Hydrogen Bonds in P-Substituted Triphenylphosphonium Cations. *J. Am. Chem. Soc.* **1994**, *116*, 968–972. (b) Agarwal, R. G.; Coste, S. C.; Groff, B. D.; Heuer, A. M.; Noh, H.; Parada, G. A.; Wise, C. F.; Nichols, E. M.; Warren, J. J.; Mayer, J. M. Free Energies of Proton-Coupled Electron Transfer Reagents and Their Applications. *Chem. Rev.* **2022**, *122*, 1–49. (c) Murray, P. R. D.; Cox, J. H.; Chiappini, N. D.; Roos, C. B.; McLoughlin, E. A.; Hejna, B. G.; Nguyen, S. T.; Ripberger, H. H.; Ganley, J. M.; Tsui, E.; Shin, N. Y.; Koronkiewicz, B.; Qiu, G.; Knowles, R. R. Photochemical and Electrochemical Applications of Proton-Coupled Electron Transfer in Organic Synthesis. *Chem. Rev.* **2021**, *122*, 2017–2291.

(21) The BDFEs of phosphonium salts were calculated according to the following equation: BDFE = 1.37 p$K_a$ + 23.06 $E_{ox}$ + $C_G$, where $E_{ox}$ is an oxidation potential of the parent ylide and $C_G$ is a constant depending on the solvent of interest. While p$K_a$ and $E_{ox}$ values measured in DMSO have been reported in ref 20a, we adopted the value of $C_G$ in DMSO ($C_G$ = 68) from ref 20b, which has been recently corrected.

(22) Wan, Y.; Zhu, J.; Yuan, Q.; Wang, W.; Zhang, Y. Synthesis of β-Silyl α-Amino Acids via Visible-Light-Mediated Hydrosilylation. *Org. Lett.* **2021**, *23*, 1406–1410.

(23) (a) Dong, J.-Y.; Xu, W.-T.; Yue, F.-Y.; Song, H.-J.; Liu, Y.-X.; Wang, Q.-M. Visible-Light-Mediated Deuteration of Aldehydes with $D_2O$ via Polarity-Matched Reversible Hydrogen Atom Transfer. *Tetrahedron* **2021**, *82*, 131946. (b) Zhang, Y.; Ji, P.; Dong, Y.; Wei, Y.; Wang, W. Deuteration of Formyl Groups via a Catalytic Radical H/D Exchange Approach. *ACS Catal.* **2020**, *10*, 2226–2230. (c) Kuang, Y.; Cao, H.; Tang, H.; Chew, J.; Chen, W.; Shi, X.; Wu, J. Visible Light Driven Deuteration of Formyl C–H and Hydridic $C(sp^3)$–H Bonds in

Feedstock Chemicals and Pharmaceutical Molecules. *Chem. Sci.* **2020**, *11*, 8912–8918.

(24) Draper, F.; Doeven, E. H.; Adcock, J. L.; Francis, P. S.; Connell, T. U. Extending Photocatalyst Activity through Choice of Electron Donor. *J. Org. Chem.* **2023**. https://doi.org/10.1021/acs.joc.2c02460.

(25) Ruffoni, A.; Mykura, R. C.; Bietti, M.; Leonori, D. The Interplay of Polar Effects in Controlling the Selectivity of Radical Reactions. *Nature Synthesis* **2022**, 1, 682–695.

(26) Seo, J. M.; Hassan, A. H. E.; Lee, Y. S. An Expeditious Entry to Rare Tetrahydroimidazo[1,5-*c*]pyrrolo[1,2-*a*]pyrimidin-7(8*H*)-ones: A Single-Step Gateway Synthesis of Glochidine Congeners. *Tetrahedron* **2019**, *75*, 130760.

(27) Zhou, X.; Yu, T.; Dong, G. Site-Specific and Degree-Controlled Alkyl Deuteration via Cu-Catalyzed Redox-Neutral Deacylation. *J. Am. Chem. Soc.* **2022**, *144*, 9570–9575.

Insert Table of Contents artwork here